Step and Flash Imprint Lithography Using UV-transparent, Electrically Conductive Templates

A. E. Hooper, A. A. Talin*, W. J. Dauksher, J. H. Baker, D. Convey, T. Eschrich, D.J. Resnick, T. C. Bailey**, S. Johnson**, and C. G. Willson**

Motorola Labs, Tempe, AZ, USA, Andy.Hooper@motorola.com
*Current address: Sandia National Labs, Livermore, CA, USA
**Texas Materials Institute, University of Texas at Austin, Austin, TX, USA

ABSTRACT

This paper presents data for the preparation and characterization of very smooth, highly transparent, sputtered indium tin oxide thin films for use in Step and Flash Imprint Lithography. Comparisons of the electrical and optical properties are presented for both the amorphous and crystalline films. Crystallization of the amorphous film by annealing results in reduction of the sheet resistance from 798 to 327 Ω/□, reduction of Hall mobility from 52.6 to 26.2 $cm^2 \cdot V^{-1} \cdot s^{-1}$, and an increase of free carrier density from 2.49×10^{19} to 1.22×10^{20} $N \cdot cm^{-3}$. The films have root-mean-square roughness values of less than 2.4 Å, and a maximum optical transmission of greater than 78% at 365 nm.

Keywords: Step and Flash Imprint Lithography, Indium Tin Oxide, Transparent Conductive Oxide.

1 INTRODUCTION

Step and flash imprint lithography (SFIL) is a promising new technique capable of resolving sub 100 nm features at a substantially lower cost than any other candidate method currently under development [1], [2], [3]. SFIL shares a common principle with other imprint lithography techniques in that a mold with an etched topography is pressed into a liquid, which then assumes the shape defined by the mold. Once the liquid is cured, the mold may be removed leaving behind the desired pattern. However, unlike imprint lithography methods which rely on thermosetting polymers, SFIL uses a transparent mold and a low-viscosity photo-curable organosilicone liquid as the pattern defining medium, thus avoiding the need for high imprinting pressures and high curing temperatures. Successful implementation of SFIL requires that the mold, or template, be highly transparent at the actinic wavelength, defect free, and be sufficiently electrically conductive such that no charging occurs during e-beam patterning to define the mold pattern or during post fabrication inspection, which requires a scanning electron microscope.

Previously, we have investigated the integration of a SiO_2/transparent conductive oxide layer into an SFIL mask structure [4]. Indium tin oxide (ITO) is a well-known transparent conductive oxide that is typically used in technologies where transparency and conductivity are of primary importance (such as in visual displays). However, for SFIL applications smoothness is very crucial because film defects and roughness can potentially transfer from the template to the pattern during imprinting. Hence, for our application we have found it necessary to first optimize the ITO smoothness before optimizing other factors such as transparency and conductivity. In this paper, we provide data for a ~600 Å thick, very smooth, highly transparent thin ITO film for use with SFIL applications. Both amorphous and crystalline films were characterized. Results for printing by a photoplate containing this film are also presented.

2 EXPERIMENTAL

ITO films were deposited at room temperature by a Motorola-designed three-cathode RF-sputter system. The geometry of the system is such that the substrate holder is located above the cathodes. The system base pressure was 5.0×10^{-7} Torr, and depositions were conducted at 3 mTorr. The substrates used were either polished quartz wafers or 2000 Å thick SiO_2-coated silicon wafer substrates. After deposition, the films were not conductive and required annealing. Annealing was performed by placing the samples directly onto a pre-heated hotplate for 3-5 minutes. Two anneal temperatures were used to yield conductive films; samples annealed at 325°C were crystalline while samples annealed at 225°C were amorphous based on x-ray diffraction (XRD) patterns.

Auger electron spectroscopy (AES) data was collected on a custom built system made from Physical Electronics Industries components. The electron beam was stationary (non rastering) with energy of 3 keV and a beam current density of approximately 0.4 mA/cm^2. Sputter etching was done with argon ions with 2 keV energy, and spectra were taken immediately after the sputtering was stopped.

Roughness data was obtained in ambient using a Digital Instruments DM3000 Atomic Force Microscope (AFM). The ITO films were imaged in tapping mode using Tapping Mode Etched Silicon Probes (Digital Instruments) that consist of a nominal tip radius of curvature of 5-10 nm.

Electrical characterization of the films was performed on a Bio-Rad Micromeasurements HL5500 Hall System.

all contacts were point contacts, and the experiments were conducted in ambient at room temperature.

XRD analysis was performed on a Siemens D5000 X-ray diffractometer employing a Gobel focusing mirror, soller slit collimator, and Cu anode.

Ultra violet/visible (UV/Vis) transmission analyses were performed using a Perkin Elmer Lambda 18 UV/Vis spectrometer. For this analysis it was necessary to prepare ITO films on smooth quartz substrates. Percent transmission curves were calculated by referencing the ITO samples to a clean quartz substrate.

3 RESULTS

Auger atomic % composition analysis for these films was performed after sputtering into the bulk of the film. Based on the peak heights and using known Auger sensitivity factors, the approximate composition of Sn dopant in the film is estimate to be 3-5%. This agrees with previously published x-ray photoelectron spectroscopic data for an identical ITO sample, which had an Sn concentration of 4.3% [4]. No significant difference was observed in the Auger scans taken on the sample before and after annealing.

Figure 1 shows XRD data for the ITO films on quartz substrates after five minute anneals at 225 and 325°C. The 225°C annealed data has no peaks, and looks identical to an unannealed film (not shown). After heating the film to 325°C, four peaks are observed at 2-theta values of 30.7, 35.5, 51.2, and 60.9° corresponding to the (222), (400), (440), and (622) orientations respectively. A previous published RHEED/XRD study describes the polycrystalline structure of ITO as a combination of (400), (222), and (440) micro-crystallite domains [5]. The additional (622) domain that we have observed is likely the result of different deposition conditions.

Table 1 lists the electrical properties of the annealed ITO films on quartz substrates. The film was not conductive prior to annealing, and the sheet resistance was $>10^6\Omega/\square$. Heating the film to 225°C for 5 minutes yielded an amorphous film with a sheet resistance of 798 $\Omega/\square$. The sheet resistance further decreased to 327 $\Omega/\square$ after heating to 325°C. After the film is crystallized at 325°C, the carrier density increases 5-fold while that Hall mobility of the film is cut in half. Decreased mobility with increasing carrier density in ITO with annealing has been previously observed [6]. This occurs because crystallization activates electron free carriers (by several possible mechanism discussed below), while electron mobility is reduced via scattering at grain boundaries or defect sites.

Figure 2 shows AFM images of the 600 Å thick ITO films on polished quartz substrates after the 225 and 325°C anneals. For both cases, the RMS roughness is less than 2.4 Å. This is comparable to the catalog roughness of Ulcoat 6025 polished quartz photoplates that are used as SFIL substrates. This value is excellent for ITO deposited at room temperature, and is comparable to ITO films prepared by pulsed laser deposition [7], [8]. After annealing at 325°C, a series of grain boundaries are observed in Fig. 2. The grain sizes appear to be less than 1000 nm in diameter. Our initial results at SFIL printing with templates containing similar ITO grain sizes suggest that these features are insignificant and do not transfer during printing (if eventually these features do become an issue, the 225°C annealed amorphous film will be a potential substitute for the process. The amorphous film lacks grain boundaries, yet still has good transparency and conductivity).

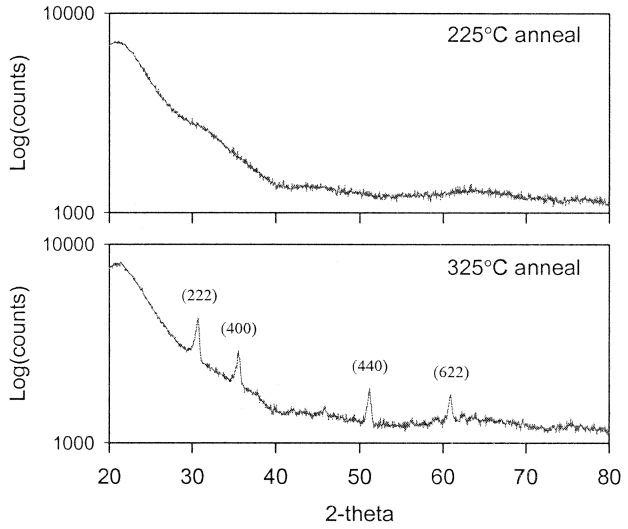

Figure 1: XRD data for ITO films on quartz substrates after five minute anneal at 225 and 325°C.

Table 1: Hall measurement data for ~600Å thick annealed ITO films on quartz substrate measured at room temperature, in ambient.

Anneal Temp.	Sheet Resist. $\Omega/\square$	Resist. $\Omega\cdot cm$	Mobility $cm^2\cdot V^{-1}s^{-1}$	Carrier Density $N\cdot cm^{-3}$
225°C	798	0.900	52.55	2.49×10^{19}
325°C	327	0.630	26.17	1.22×10^{20}

Figure 3 shows the UV-Vis transmission spectra for the ITO films on quartz after annealing. The transparency in the visible region is very good for both the amorphous and crystalline films, and drops off rapidly in the UV-region below 200 nm (this is primarily due to the ITO, not the quartz substrate). Although Fig. 3 shows that the annealed ITO film is >78% transparent at 365 nm, we plan to show in a future publication that the transparency can be >90% at 365 nm by slightly increasing the ITO thickness to ~800Å, and by using more controlled anneal conditions.

To demonstrate our initial success, Figure 4a shows a scanning electron microscope (SEM) image of an etch barrier after imprinting with an ITO-based SFIL template. Semi-isolated 20 nm lines with 150 nm spaces were successfully imprinted, and these represent the smallest features present on the starting (ITO-modified) template shown in Figure 4b. Sub-100 nm features were found to measure approximately 15 nm over coded sizes on the template. Within the noise of the SEM, the final imprinted images were found to be identical in size (e. g., no imprinting bias) to those found on the templates. Excellent imprint uniformity was also observed.

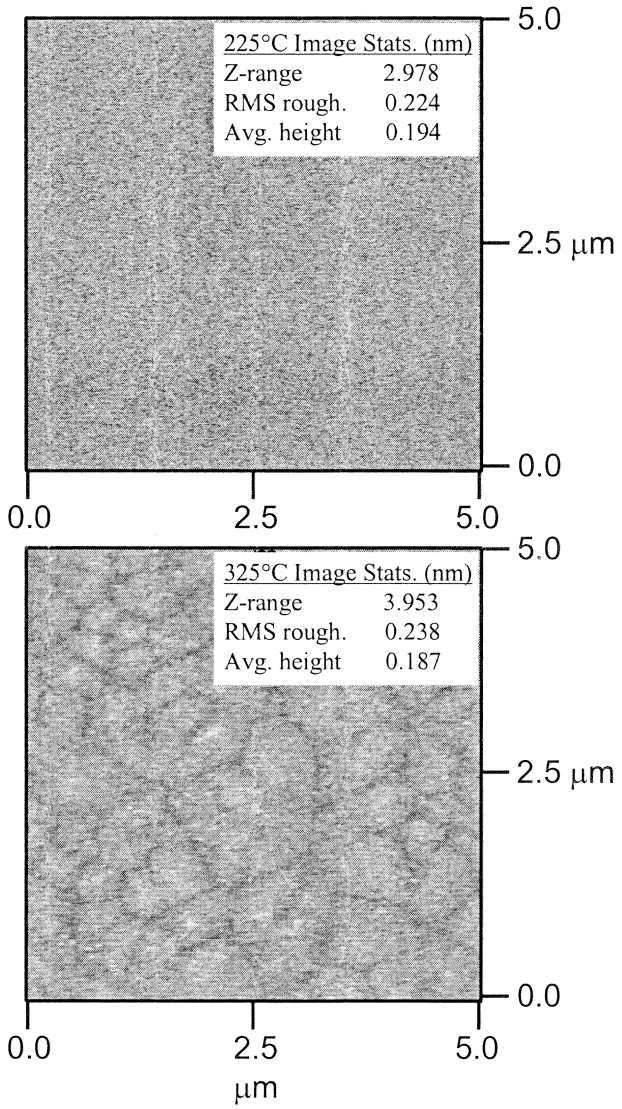

Figure 2: AFM images of the 600 Å thick ITO films on polished quartz substrates after the 225 and 325°C anneals.

4 DISCUSSION

For the ITO films described in this paper, we observed that electron free carrier mobility decreased with increasing carrier density after the ITO was crystallized. The conduction mechanism in ITO is not straightforward, and several detailed mechanisms have been proposed by previous publications [9], [10], [11], [12]. In general, In_2O_3 becomes an n-type conductor by doping with metal ions having a higher valence than indium. Free electron carriers can be generated by direct doping by Sn atoms, the reduction of inactive Sn donors by the removal of interstitial oxygen, and by oxygen vacancies acting as electron donors. In particular, the conductivity of ITO increases with the activation of Sn^{4+} dopants. Carrier mobility is affected by the degree of electron "scattering", and the literature provides several possible scattering mechanisms in ITO [11], [12], [13], [14], [15]. This includes scattering at grain boundaries, by acoustical phonons, and by both charged and uncharged defect sites. There is much debate over which kind of scattering is dominant for ITO prepared under various conditions. For example, some researchers have shown that carrier concentration and mobility in ITO can be optimized by carefully controlling ITO density and grain size [16]. However, other researchers believe that scattering from ionized atomic centers (e.g. Sn^{4+}) is dominant, and suggest that electron mobility and density are mutually opposed [12].

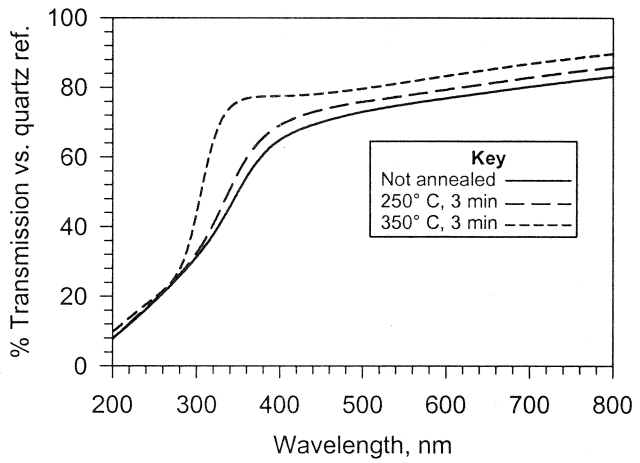

Figure 3: UV-Vis % transmission spectra for the ~600 Å thick ITO film on a quartz substrate after annealing at different temperatures.

5 CONCLUSION

We have demonstrated a ~600Å thick sputtered ITO film that can be successfully incorporated into a SFIL quartz photoplate mask structure. These films are extremely smooth and highly transparent in the region of interest. By Auger analysis, the Sn dopant concentration was 3-5%. After annealing, the ITO film sheet resistance was sufficient to act as a charge dissipation layer for SEM analysis for both amorphous and crystalline films. Crystallization of the ITO by annealing at 325°C caused

reduction of the film's sheet resistance, reduction of the Hall mobility, and increased the free carrier density. The 325°C-annealed films were found to be polycrystalline by XRD. The ITO films have an AFM measured RMS roughness of less than 2.4 Å. The optical transmission improves with anneal temperature, and at 365 nm the optical % transmission was greater than 78% after annealing at 325°C for 5 minutes.

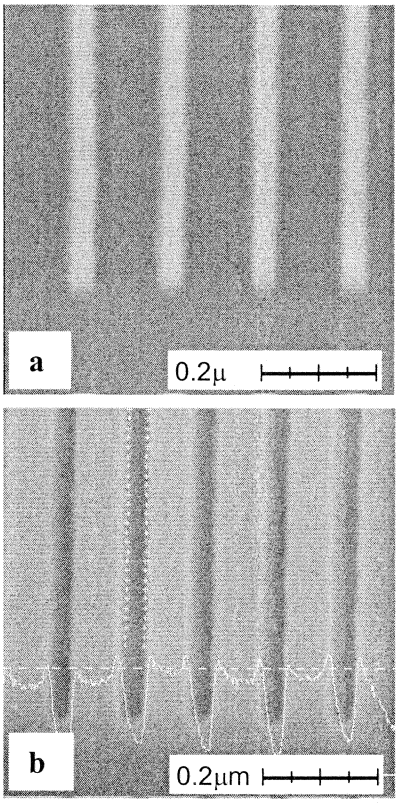

Figure 4: a) SEM Image in the etch barrier after imprinting with an ITO-based SFIL template. Shown are 20 nm lines / 150 nm spaces. b) Semi-isolated 20 nm features on an SFIL mask containing the ITO layer.

ACKNOWLEDGEMENTS

We gratefully acknowledge Yi Wei, David Mancini, and Kevin Nordquist for providing background information and insightful discussions. We would also like to thank David Standfast for etch processing support and Anne Dinsmore of Motorola's DigitalDNA™ Laboratories providing SEM analysis. In addition, we would like to thank, the support of the staff of Motorola Lab's Physical Sciences Research Laboratories for SFIL template fabrication. We would also like to thank S. V. Sreenivasan, Byung Jin Choi, Matthew Colburn, and the rest of the University of Texas at Austin's SFIL team for their help in SFIL equipment and process development. Finally, it should be noted that this work was funded in part by DARPA (BAA 01-08/01-8964 and MDA972-97-1-0010) and SRC (96-LC-460).

REFERENCES

[1] M, Colburn, T. Bailey, B.J. Choi, J.G. Ekerdt, S.V. Sreenivasan, C.G. Willson, Solid State Technology, 46(7), 67, 2001.

[2] T. Bailey, B.J. Choi, M. Colburn, M. Meissl, S. Shaya, J.G. Ekerdt, S.V. Sreenivasan, C.G. Wilson, Journal of Vacuum Science and Technology B, 18(6), 3572-3577, 2000.

[3] D.J. Resnick, D.P. Mancini, S.V. Sreenivasan, G. Wilson, Semiconductor International, June 1, 71-80, 2002.

[4] W.J. Dauksher, K.J. Nordquist, D.P. Mancini, D.J. Resnick, J.H. Baker, A.E. Hooper, A.A. Talin, T.C. Bailey, A.M. Lemonds, S.V. Sreenivasan, J.G. Ekerdt, C.G. Willson , To be published in The Journal of Vacuum Science and Technology: Proceedings of the 46th International Conference on Electron, Ion and Photon Beam Technology & Nanofabrication 2002.

[5] K. Masayuki, Y. Shigesato, S. Takaki, Thin Solid Films, 259, 38-45, 1995.

[6] H. Morikawa, M. Fujita, Thin Solid Films, 339, 309-313, 1999.

[7] V. Craciun, D. Craciun, Z. Chen, J. Hwang, R.K. Singh, Materials Research Society Symposium Series, 617, J3.13.1-J3.13.6, 2000.

[8] H. Kim, J.S. Horwitz, A. Piqué, C.M. Gilmore, D.B. Chrisey, Applied Physics A, 69(suppl.), S447-S450, 1999.

[9] A.J. Freeman, K.R. Poeppelmeier, T.O. Mason, R.P.H. Chang, T.J. Marks, MRS Bulletin, 25(8), 45-51, 2000.

[10] C.H.L. Weijtens, Journal of the Electrochemical Society, 138(11), 3432-3434, 1991.

[11] G. Frank, H. Köstlin, Applied Physics A, 27, 197-206, 1982.

[12] G. Franz, B. Lange, S. Sotier, Journal of Vacuum Science and Technology A, 19(5), 2514-2521, 2001.

[13] I. Hamberg, C.G. Granqvist, Journal of Applied Physics, 60(11), R123-R159, 1986.

[14] T.J. Coutts, D.L. Young, X. Li, MRS Bulletin, 25(8), 58-65, 2000.

[15] A.K. Kulkarni, S.A. Knickerbocker, Journal of Vacuum Science and Technology A, 14(3), 1709-1713, 1996.

[16] S.K. Choi, J.I. Lee, Journal of Vacuum Science and Technology A, 19(5), 2043-2047, 2001.